HHS Public Access

Author manuscript

J Solgel Sci Technol. Author manuscript; available in PMC 2020 August 27.

Published in final edited form as:

J Solgel Sci Technol. 2019 ; 91(1): 11–20. doi:10.1007/s10971-019-04995-4.

Synthesis of silica-alginate nanoparticles and their potential application as pH-responsive drug carriers

Xin Fan[1], **Roman C. Domszy**[2], **Naiping Hu**[3], **Arthur J. Yang**[3], **Jeff Yang**[3], **Allan E. David**[1,*]

[1]Department of Chemical Engineering, Auburn University, Auburn, AL

[2]Industrial Science & Technology Network, Inc., Lancaster, PA

[3]Lynthera Corporation, Lancaster, PA

Abstract

Composite silica-alginate nanoparticles were prepared via silica sol-gel technique using a water-in-oil microemulsion system. In our system, cyclohexane served as the bulk oil phase into which aqueous solutions of sodium alginate were dispersed as droplets that confined nanoparticle formation after addition of tetraethylorthosilicate (TEOS). Our studies showed that much of the particle growth is completed within the first 24 hours and reaction times up to 120 hours only resulted in an additional 5% increase in particle diameter. Average particle size was found to decrease with increasing water-to-surfactant molar ratio (*R*) and with increasing cocentration of alginate in the aqueous phase. The potential for drug loading during particle formation was demonstrated using rhodamine B as a model drug. *In vitro* release studies showed that particles incubated in pH 2.5 phosphate buffer released only about 7% of the drug load in 27 days, while 42% was released in pH 7.5 phosphate buffer over the same period. Analysis of the release profile suggested that rhodamine B was homogeneously distributed throughout the particle and that the drug diffusivity was 40-fold greater in pH 7.5 buffer compared to that at pH 2.5. These results suggest that silica-alginate nanoparticles could be used as a pH-responsive drug carrier for controlled drug release.

Graphical Abstract

The inclusion of a Graphical Abstract (GA) is mandatory. It should be supplied at the time the manuscript is first submitted and accompanied by a detailed caption describing the GA. The graphical abstract helps readers to determine the content and importance of the manuscript at a glance. Graphical abstracts should consist of carefully drawn figures (chemical structures, charts, graphs, or other informative illustration) that show the most striking feature of the article in a pictorial form. The figure(s) in the graphical abstract must meet the same quality and permissions standards as any other figure in the article. Compound numbers can be given in the graphical

*Corresponding author: aedavid@auburn.edu; telephone 334-844-8119.

Conflicts of interest

There are no conflicts to declare.

abstract if they refer to a graphic also shown there. The use of color to enhance the value and quality of the graphic is encouraged.

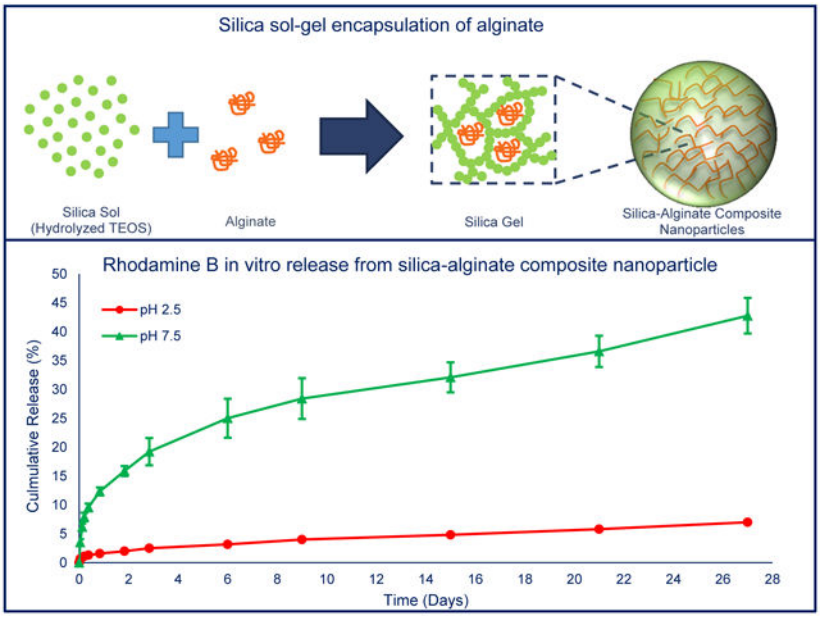

Composite nanoparticles were formed by entrapment of alginate within silica sol-gel nanoparticles. These nanoparticles showed pH-dependent *in vitro* release profile of rhodamine B in phosphate buffers (pH 2.5 or pH 7.5). At pH 2.5, a 7 % cumulative release of rhodamine B was observed over 27 days, while 42 % cumulative release was observed at pH 7.5

Keywords

silica-alginate nanoparticles; sol-gel encapsulation; microemulsion; pH-responsive drug release; rhodamine B

1. Introduction

Silica sol-gel techniques, which involve the hydrolysis and polycondensation of a silica precursor, have been used to encapsulate a variety of polysaccharides to produce silica-polysaccharide composite materials [1, 2]. Polysaccharides that have been utilized include alginate, chitosan, carrageenan, and cellulose [3], with alginate among the most studied [4]. Alginate, which is extracted primarily from the cell wall of brown algae, is a water soluble, anionic polysaccharide with a chemical structure that consists of a mixture of poly-β-1,4-D-mannuronic acid (M units) and α-1,4-L-glucuronic acid (G units) in various proportions [5]. It is biocompatible and biodegradable and has been widely used as an additive in food products and as a support for enzyme- or cell-based biocatalysts and bioreactors [6, 7]. Hydrogels of alginate have also been studied for applications in wound healing, artificial organs, and pH-responsive drug delivery systems [8-10].

Silica-alginate composite materials have attracted attention because of the potential for enhanced collective properties obtained by contributions from each individual component [3]. Silica has been utilized because of its good physical and chemical stability as well as its acceptable biocompatibility [11]. Moreover, silica does not substantially alter the optical or magnetic properties of components with which it is combined [12]. Finally, hydroxyl groups on the surface of silica particles allow for facile chemical surface modifications and introduction of functional groups [13]. Silica particles can also be used for controlled release applications, with release profiles tailored by controlling the pore volume, pore size and tortuosity, and surface chemistry on the particle [14].

Several methods have been utilized to produce silica-alginate composite materials, including: 1) coating alginate hydrogels with silica [15]; 2) simultaneous gelation of a mixture of alginate and silica [16]; or by 3) adding silica particles into an alginate solution prior to gelation [17]. Regardless of synthesis method, most of the reported composite materials were in the form of large beads, bulk gels, films or fibers and only a few studies have reported on nanosized silica-alginate composite particles. For example, silica-alginate nanoparticles as hybrid capsules have been synthesized via the spray drying method [18, 19], and alginate coated mesoporous silica nanoparticles have been studied as drug carriers [20, 21]. In this work, we utilized a sol-gel technique and water-in-oil microemulsion method for synthesis of silica-alginate composite nanoparticles. Sol-gel synthesis has also been applied with water-in-oil microemulsions systems for synthesis of nano-sized silica-based composites of varying structure and composition [22].

Water-in-oil microemulsion reactions consist of a bulk oil phase with suspended water droplets, often stabilized with surfactants, that serve as reactors for nanoparticle synthesis [23]. In many instances, the silica sol-gel precursor (e.g. tetraethyl orthosilicate - TEOS) is initially found in the oil phase but then diffuses into the water droplets, after hydrolysis, where it co-condenses with other hydrolyzed precursors to form particles. Any component located in the water droplet, prior to addition of TEOS, can be encapsulated inside the growing silica framework [24]. The final structure and size of the nanocomposite particles can be controlled by varying microemulsion parameters (e.g. concentrations, surfactant, temperature, etc.) [25].

The current state of development of nanoparticle-based drug delivery systems has been extensively reviewed in the literature [26-28]. Various nanoparticles have been studied as drug delivery systems, such as polymeric nanoparticles, liposomes, metallic nanoparticles, and dendrimers [29, 30]. Advantages offered compared to conventional drug delivery systems, include improved bioavailability and biodistribution, lower toxicity, and targeted drug delivery [31]. With a number of parameters that could be varied, including particle size, shape, and composition, to meet the requirements of different drug delivery strategies, nanoparticles offer enormous potential for improving therapeutic efficacy of drugs. However, the large parameter space of particle properties is so large that much work remains to be done in understanding the relationship between particle properties and treatment efficacy.

In this study, we demonstrated the synthesis of silica-alignate nanoparticles using the versatile microemulsion technique and tested the potential of the nanoparticles as pH-responsive drug carriers. Alginate, which provides pH-responsive functionality, was encapsulated within a silica network, which provided mechanical integrity. The effect of synthesis parameters on particle size and composition were studied by varying the water-to-surfactant molar ratio and the initial concentration of alginate. Finally, the pH-dependent release of rhodamine B, as a model drug, from the composite was evaluated. This work describes an avenue for the synthesis of composite silica-alginate nanoparticles, which offers potential as a “smart”, pH-controlled drug delivery vehicle.

2. Experimental

2.1 Materials

Sodium alginate was purchased from Acros (New Jersey, USA); tetraethyl orthosilicate (98% purity) was purchased from Sigma Aldrich (Missouri, USA); Triton X-100 and rhodamine B were purchased from AMRESCO (Ohio, USA); cyclohexane, ethanol, aqueous ammonia solution (29 wt.% ammonia), isopropyl alcohol (70%), hydrochloric acid (37%), and sulfuric acid were purchased from BDH Chemicals (Pennsylvania, USA). Sodium alginate (very low viscosity) and n-hexanol, were purchased from Alfa Aesar (Massachusetts, USA). All chemicals were used as provided without further purification. Deionized (DI) water was obtained from an Elga Purelab Flex water purification system (Veolia Water Technologies, UK).

2.2 Synthesis of composite silica-alginate nanoparticles by water-in-oil microemulsion

For a typical preparation of silica-alginate nanoparticles, 16.8 mL n-hexanol was mixed with 60 mL cyclohexane, followed by addition of 4 mL alginate solution (0.05% w/v) with vigorously stirring at room temperature. After 5 minutes, 14 mL Triton X-100 was added dropwise and the mixture was observed to become optically transparent. After 10 minutes of vigorous stirring, 1 mL TEOS was added, followed by the addition of 500 μL aqueous ammonia solution (29 wt.%) after 5 minutes. The reaction was allowed to continue for 24 hours at room temperature under stirring and then 100 mL acetone was added to break the stability of the microemulsion. Precipitated particles were collected by centrifugation (4500 rpm, 10 minutes) and then washed, two times with isopropyl alcohol and once with DI water, to remove the excess surfactants and co-surfactants. Particles were stored in DI water at 4 °C until use.

To determine the effect of reaction time on nanoparticle synthesis, aliquots (2 mL) of the microemulsion were taken at 24, 48, 72, 96, and 120 hours for particle size measurement by transmission electron microscopy. The effects of water-to-surfactant ratio and alginate concentration on nanoparticle size were determined while keeping all other parameters constant.

2.3 Determination of composition by thermogravimetric analysis

Thermogravimetric analysis (TGA) was performed, with a TA-500 thermogravimetric analyzer (TA Instruments, Delaware, USA), after nanoparticles were first lyophilized for 24

hours to remove bulk water. Experiments were carried out in a flowing air (40 mL/min) atmosphere with isothermal conditioning at 120 °C for 20 minutes, to remove residual water and other volatiles, followed by a heating rate of 10 °C/min up to 900 °C.

2.4 Imaging of nanoparticles by transmission electron microscopy

A Zeiss (Oberkochen, Germany) EM 10 Transmission Electron Microscope (TEM) operating at a voltage of 60 kV was used to determine the size of the nanoparticles. TEM samples were prepared by placing a single drop of silica-alginate nanoparticle suspension on a carbon type B, 300 mesh grid and placing the grid in a petri dish and allowing it to dry at ambient conditions.

2.5 Loading and *in vitro* release study of rhodamine B from nanoparticles

Rhodamine B was loaded into the silica-alginate nanoparticles by its addition into the water-in-oil microemulsion prior to particle formation. Rhodamine B (1 mg/mL) was first dissolved in the sodium alginate aqueous solution (very low viscosity, 5 % w/v). The composite particles were then synthesized by mixing 60 mL cyclohexane, 20 mL n-hexanol, 6 mL alginate solution with rhodamine B, 25 mL Triton X-100, 1 mL TEOS and 500 μL aqueous ammonia solution (29 wt%). Rhodamine B loaded composite particles were collected by centrifugation (4500 rpm, 10 minutes) and washed two times with isopropyl alcohol and once with DI water.

In vitro drug release was measured by dispersing rhodamine B-loaded nanoparticles in 1 mL phosphate buffer (10 mM; pH 2.5 or pH 7.5). At predetermined time intervals, samples were centrifuged at 14,800 rpm for 5 minutes before 0.5 mL supernatant was removed for analysis and 0.5 mL of fresh phosphate buffer added back to the vial. The amount of rhodamine B released was measured using a Molecular Devices FlexStation 3 fluorescence spectrophotometer (excitation: 542 nm, emission: 582 nm) and concentrations determined using a calibration curve of known rhodamine B concentrations. After 27 days, all nanoparticles were dissolved in 1 mL sodium hydroxide (1 M) to measure any residual rhodamine B remaining inside the nanoparticles. All nanoparticle samples were analyzed in triplicate (n = 3) and results reported as the mean ± standard deviation.

3. Results and Discussion

An illustration of the water-in-oil microemulsion synthesis of silica-based composite particles by sol-gel encapsulation is shown in Fig. 1. In our system, cyclohexane served as the bulk oil phase, TX-100 was used as surfactant, n-hexanol served as a co-surfactant, and aqueous solutions of sodium alginate formed the water phase droplets.

3.1 Effect of reaction time on nanoparticle size

It has been reported that increasing reaction time leads to the production of larger silica nanoparticles [34, 35]. We, therefore, first monitored the change in particle size with reaction times ranging from 24 to 120 hours using the formulation listed in Table 1. Analysis of TEM images, examples shown in Fig. 2, showed that particles were spherical in shape and monodisperse with average sizes of 73.4 ± 2.3 nm at 24 hours; 75.9 ± 3.5 nm at 48

hours; 76.7 ± 2.8 nm at 72 hours; 79.4 ± 2.1 nm at 96 hours; and 77.2 ± 1.8 nm at 120 hours. Since more than 90% of particle growth occurred during the first 24 hours, all subsequent reaction times were fixed at 24 hours.

3.2 Variation of the alginate-to-silica ratio in composite nanoparticles

To determine if the alginate content within the nanoparticles could be varied, particles were synthesized with varying alginate concentrations, as listed in Table 2, and characterized with thermogravimetric analysis (TGA). The TGA and DTGA (first derivative TGA) curves of sodium alginate alone, presented in Fig. 3A, showed that alginate has two decomposition steps, between 200-300 °C and 500-600 °C, that result in a 85% weight loss up to 900 °C; leaving mostly sodium carbonate residue [36]. Particles comprised of only silica, on the other hand, showed a total weight loss of 5%, as shown in see Fig. 3B, with an initial dehydration step followed by weight loss occurring between 400-600 °C due to the condensation of surface and internal hydroxyl groups [37]. For composite silica-alginate nanoparticles produced with initial alginate concentrations of 0.1, 0.5, and 1% w/v, the decomposition steps were similar to those of sodium alginate and the total weight loss was 9.5, 10.7 and 13.1 wt.%, respectively, as shown in Fig. 3C. To determine the alginate content, a mass balance, with 100 mg of silica-alginate composite as a basis, was established as,

$$100\,W_t = aW_{SA} + (100 - a)W_{Silica}$$

where is the total weight loss by the composite nanoparticles, is the weight loss by silica nanoparticles (i.e. 5%), and is the sodium alginate weight loss (i.e. 85%). This equation can be solved for the percentage of alginate (a) in the composite nanoparticles, which is calculated as,

$$a = 100\frac{w_t - w_{Silica}}{w_{SA} - w_{Silica}}$$

Based on this analysis, particles synthesized with 0.1, 0.5, and 1.0% w/v alginate solutions showed alginate content of 5.6, 7.1, and 10.1 wt.%, respectively. These results confirmed the successful utilization of the water-in-oil emulsion for integration of alginate within silica nanoparticles formed by the sol-gel reaction. It also demonstrated that the amount of alginate could be varied by changing the concentration of alginate solution used in the synthesis. It should be noted, however, that the range of alginate:silica ratio obtained in this study was limited somewhat by the rapid viscosity increase with higher alginate concentrations. This could potentially be overcome by utilizing alginates with a lower molecular weight, as the viscosity has been shown to be linearly related to the degree of polymerization [38].

3.3 Evaluation of the effect of water-to-surfactant ratio (*R*) on particle size

The water-to-surfactant ratio was varied, while keeping all other parameters constant, to determine its effect on the size of silica-alginate nanoparticles. Fig. 4 shows that all particles

retained a spherical shape and analysis of size distribution, summarized in Table 3, shows that particle size increased with decreasing *R*-value. The *R*-ratio affects several parameters in water-in-oil microemulsions, including the size of water droplets, the ratio of bulk-water to bound-water molecules, the number of reactive silica monomers per water droplet, the rigidity of the surfactant-water interface, and the dynamics of intermicellar interaction [39-41]. The formation of silica based nanoparticles in water-in-oil microemulsion includes a nucleation step and growth of the nucleus into particles by the addition of reactive monomers. The relatively higher surfactant concentration at low *R* values leads to a greater number of water droplets and, therefore, a higher rate of intermicellar collisions [33]. This process would presumably redistribute the reactive silica monomers across droplets, keeping the concentration below the nucleation threshold and lowering the nucleation rate. The smaller number of nuclei formed and abundance of silica monomers available for particle growth leads to particles of greater average size [32].

Comparing the particles in Fig. 4 to those presented in Fig. 2, there is a clear difference in particle size. This size difference could due to the change in molar ratio of water to TEOS ratio (***h***). The nanoparticles in Fig. 2 were produced under conditions with $h = 24.8$ while a $h = 49.6$ was used for those in Fig. 4. An increase in ***h*** results in greater availability of water for hydrolysis of TEOS, it increases the stability of hydrolyzed silica species and it also extends the duration of the particle nucleation [34]. This leads to an increase in the number of nuclei and formation of particles of smaller size due to the mass balance.

3.4 Effect of alginate concentration on size of composite nanoparticles

The effect of alginate concentration on the size of composite particles was also studied. Analysis of TEM images (Fig. 5) shows that smaller particles were produced as alginate concentration was increased (Table 4). This could be due to interactions between alginate and the flexible surfactant layers producing changes in droplet elasticity, shape and rheological properties [42]. Potential fluctuations of dispersed droplet properties, driven by alginate in the water droplet, may destabilize larger domains and produce smaller droplets with a larger surface to volume ratio [43]. As a result, more TEOS associates with water droplets and the increased hydrolysis rate produces a greater number of nuclei, and eventually smaller size particles [32, 33]. Studies that monitor silica concentrations in the different domains and changes in domain sizes could yield further insight into the process of particle formation.

3.5 Demonstration of pH-responsive release of rhodamine B

Rhodamine B, as a model, hydrophilic drug, was loaded into the composite nanoparticles by silica sol-gel encapsulation to study its pH-depencdent *in vitro* release. While the drug loading was relatively low (~0.3 %), likely due to leaching during the extensive washing procedure, the release of rhodamine B could still be monitored by measuring fluorescence intensities. co Fig. 6 shows the cumulative release percent of rhodamine B from silica-alginate nanoparticles in pH 2.5 and pH 7.5 phosphate buffers. Over a period of 27 days, only 7% of loaded rhodamine B was released when particles were incubated in pH 2.5 phosphate buffer. However, approximately 42% of loaded rhodamine B was released in pH 7.5 phosphate buffer over the same period.

While the mechanism driving the observed pH-dependent drug release behavior is yet to be clearly elucidated, we hypothesize that favorable hydrogen bonding between alginate (pKa 3.2) and rhodamine B (pKa 3.1 - 4.2), which would both have protonated carboxylic acid groups under acidic conditions, resulted in the limited release from silica-alginate nanoparticles at pH 2.5. At pH 7.5, on the other hand, the deprotonated carboxylic acid groups are negatively charged, which leads to electrostatic repulsion and, thus, release of rhodamine B from the particles. Future studies will evaluate the contribution of hydrogen bonding in modulating drug release by utilizing chemical modification of alginate function groups and other polysaccharides.

Fitting of the rhodamine B release data to mathematical models was used to obtain insights of the underlying mass transport processes, which might include the diffusion of water into the particle, swelling of the polymer, matrix erosion, drug diffusion or dissolution, and other phenomena [44]. The semi-empirical Peppas equation, which assumes a perfect sink condition for release of the first 60% of drug [45], is expressed as,

$$\frac{M_t}{M_\infty} = kt^n$$

where is the cumulative amount of drug released in time t, is the cumulative amount of drug released at infinite time, k is a constant related to device structure and geometry, and exponent n is used to characterize the release mechanism.

For spherical systems, $n = 0.43$ corresponds to a Fickian diffusion mechanism (diffusion-controlled release), $0.43 < < 0.85$ to anomalous transport (both diffusion-controlled and erosion controlled release), and $n = 0.85$ to Case II transport (zero-order release) [40], It has been suggested in literature that < 0.43 also represents Fickian diffusion [47-49]. Fitting of the Peppas equation to the data using MATLAB 2017b (MathWorks), as shown in Fig. 7A, yield $n = 0.42$ for pH 2.5 and $n = 0.35$ for pH 7.5 phosphate buffer, suggesting Fickian diffusion in both cases.

For diffusion controlled systems, a monolithic solution model [50], can be used for early time ($\frac{M_t}{M_\infty} < 0.4$) to study the drug distribution inside the system with following correlation,

$$\frac{M_t}{M_\infty} = 6\left(\frac{Dt}{\pi r^2}\right)^{\frac{1}{2}} - \frac{3Dt}{r^2}$$

where is the cumulative amount of drug released in time t, is the cumulative amount of drug released at infinite time, D is the diffusion coefficient, and r is the radius of the sphere (r nm from TEM images).

The monolithic solution model provided good fits with experimental data obtained in both phosphate buffer solutions, as shown in Fig. 7B. This implies that rhodamine B was homogeneously distributed throughout the particles by the microemulsion process. In addition, the diffusion coefficient in pH 7.5 phosphate buffer was found to be 40 times

greater than that at pH 2.5. The apparent low diffusion coefficient at pH 2.5 may be due to hydrogen bonding between -COOH groups in alginate and rhodamine B while electrostatic repulsion could enhance release at pH 7.5, as previously stated. It is also possible that increased solvation of alginate at the higher pH leads to a more open structure for rhodamine B diffusion, while the opposite is true at the low pH. Further experiments are required to more clearly elucidate the mechanism of the observed pH-dependent release. Since the monolithic solution model suggests that the drug release rate from silica-alginate nanoparticles is a function of the ratio D/r^2, which can be tailored by modifying the synthesis conditions as described above, this suggests the potential to modulate drug release by proper engineering of nanoparticle composition and size. Future studies are required to more clearly elucidate the mechanism of the pH-dependent release.

4. Conclusions

In this work we describe the use of a microemulsion method for the synthesis of composite silica-alginate nanoparticles which, to the extent of our knowledge, has not been previously reported. Encapsulation of alginate in the composite nanoparticles was confirmed by TGA, and the weight ratio of alginate controlled by initial alginate solution concentration. Furthermore, we demonstrated that the size of silica-alginate nanoparticles was controlled by changing the water to surfactant molar ratio or initial alginate concentration. With rhodamine B as a model drug, the silica-alginate composite nanoparticles displayed release kinetics that was pH-dependent, showing significantly greater release at pH 7.5 compared to pH 2.5. Evaluation of the release profiles suggested that drug transport was governed by Fickian diffusion and that the rhodamine B was homogenously distributed throughout the nanoparticle. While additional studies are required to elucidate the mechanisms of pH-dependent release, this composite nanoparticle offers potential as a drug carrier with pH-sensitive triggering of drug release (e.g. for oral drug delivery that utilizes pH variation through the gastric tract). Versatility of the synthesis method also allows for optimization of particle composition and size for specific drug delivery applications.

References

1. Ciriminna R, Sciortino M, Alonzo G, Schrijver Ad, Pagliaro M (2011) From Molecules to Systems: Sol–Gel Microencapsulation in Silica-Based Materials. Chem Rev 111 (2):765–789 [PubMed: 20726523]
2. Shchipunov YA, Karpenko TyY (2004) Hybrid Polysaccharide–Silica Nanocomposites Prepared by the Sol–Gel Technique. Langmuir 20 (10):3882–3887 [PubMed: 15969374]
3. Singh V, Srivastava P, Singh A, Singh D, Malviya T (2016) Polysaccharide-Silica Hybrids: Design and Applications. Polym Rev 56 (1): 113–136
4. Coradin T, Livage J (2003) Synthesis and Characterization of Alginate/Silica Biocomposites. J Sol-Gel Sci Technol 26 (1): 1165–1168
5. Pawar SN, Edgar KJ (2012) Alginate derivatization: A review of chemistry, properties and applications. Biomaterials 33 (11):3279–3305 [PubMed: 22281421]
6. Wylie A (1973) Alginates as Food Additives. Royal Society of Health Journal 93 (6):309–313 [PubMed: 4793739]
7. Mohamad NR, Marzuki NHC, Buang NA, Huyop F, Wahab RA (2015) An overview of technologies for immobilization of enzymes and surface analysis techniques for immobilized enzymes. Biotechnol Biotechnol Equip 29 (2):205–220 [PubMed: 26019635]

8. Boateng JS, Matthews KH, Stevens HNE, Eccleston GM (2008) Wound healing dressings and drug delivery systems: A review. J Pharm Sci 97 (8):2892–2923 [PubMed: 17963217]
9. Lee KY, Mooney DJ (2012) Alginate: Properties and biomedical applications. Prog Polym Sci 37 (1): 106–126 [PubMed: 22125349]
10. Jain D, Bar-Shalom D (2014) Alginate drug delivery systems: application in context of pharmaceutical and biomedical research. Drug Dev Ind Pharm 40 (12): 1576–1584 [PubMed: 25109399]
11. Jaganathan H, Godin B (2012) Biocompatibility assessment of Si-based nano- and micro-particles. Adv Drug Deliv Rev 64 (15): 1800–1819 [PubMed: 22634160]
12. Vivero-Escoto JL, Huxford-Phillips RC, Lin W (2012) Silica-based nanoprobes for biomedical imaging and theranostic applications. Chem Soc Rev 41 (7):2673–2685 [PubMed: 22234515]
13. McCarthy SA, Davies G-L, Gun'ko YK (2012) Preparation of multifunctional nanoparticles and their assemblies. Nat Protoc 7 (9): 1677–1693 [PubMed: 22899335]
14. Barbé CJ, Kong L, Finnie KS, Calleja S, Hanna JV, Drabarek E, Cassidy DT, Blackford MG (2008) Sol-gel matrices for controlled release: from macro to nano using emulsion polymerisation. J Sol-Gel Sci Technol 46 (3):393–409
15. Heichal-Segal O, Rappoport S, Braun S (1995) Immobilization in Alginate-Silicate Sol-Gel Matrix Protects β-Glucosidase Against Thermal and Chemical Denaturation. Biotechnology 13 (8): 798–800
16. Kawakami K, Furukawa S-Y (1997) Alcohol-oxidation activity of whole cells ofpichia postons entrapped in hybrid gels composed of Ca-alginate and organic silicate. Appl Biochem Biotechnol 67 (1):23–31
17. Fukushima Y, Okamura K, Imai K, Motai H (1988) A new immobilization technique of whole cells and enzymes with colloidal silica and alginate. Biotechnol Bioeng 32 (5):584–594 [PubMed: 18587759]
18. Boissière M, Allouche J, Chanéac C, Brayner R, Devoisselle J-M, Livage J, Coradin T (2007) Potentialities of silica/alginate nanoparticles as Hybrid Magnetic Carriers. Int J Pharm 344 (1–2): 128–134 [PubMed: 17611055]
19. Boissiere M, Meadows PJ, Brayner R, Helary C, Livage J, Coradin T (2006) Turning biopolymer particles into hybrid capsules: the example of silica/alginate nanocomposites. J Mater Chem 16 (12):1178–1182
20. Hu L, Sun C, Song A, Chang D, Zheng X, Gao Y, Jiang T, Wang S (2014) Alginate encapsulated mesoporous silica nanospheres as a sustained drug delivery system for the poorly water-soluble drug indomethacin. Asian J Pharm Sci 9 (4): 183–190
21. Feng W, Nie W, He C, Zhou X, Chen L, Qiu K, Wang W, Yin Z (2014) Effect of pH-Responsive Alginate/Chitosan Multilayers Coating on Delivery Efficiency, Cellular Uptake and Biodistribution of Mesoporous Silica Nanoparticles Based Nanocarriers. ACS Appl Mater Interfaces 6 (11):8447–8460 [PubMed: 24745551]
22. Wang J, Shah ZH, Zhang S, Lu R (2014) Silica-based nanocomposites via reverse microemulsions: classifications, preparations, and applications. Nanoscale 6 (9):4418–4437 [PubMed: 24562100]
23. López-Quintela MA (2003) Synthesis of nanomaterials in microemulsions: formation mechanisms and growth control. Curr Opin Colloid Interface Sci 8 (2): 137–144
24. Wang J, Tsuzuki T, Sun L, Wang X (2010) Reverse Microemulsion-Mediated Synthesis of SiO2-Coated ZnO Composite Nanoparticles: Multiple Cores with Tunable Shell Thickness. ACS Appl Mater Interfaces 2 (4):957–960 [PubMed: 20423116]
25. Arriagada FJ, Osseo-Asare K (1999) Synthesis of Nanosize Silica in a Nonionic Water-in-Oil Microemulsion: Effects of the Water/Surfactant Molar Ratio and Ammonia Concentration. J Colloid Interface Sci 211 (2):210–220 [PubMed: 10049537]
26. Parveen S, Misra R, Sahoo SK (2012) Nanoparticles: a boon to drug delivery, therapeutics, diagnostics and imaging. Nanomedicine 8 (2): 147–166 [PubMed: 21703993]
27. Blanco E, Shen H, Ferrari M (2015) Principles of nanoparticle design for overcoming biological barriers to drug delivery. Nat Biotechnol 33:941–951 [PubMed: 26348965]
28. Chen G, Roy I, Yang C, Prasad PN (2016) Nanochemistry and Nanomedicine for Nanoparticle-based Diagnostics and Therapy. Chem Rev 116 (5):2826–2885 [PubMed: 26799741]

29. Wilczewska AZ, Niemirowicz K, Markiewicz KH, Car H (2012) Nanoparticles as drug delivery systems. Pharmacol Rep 64 (5): 1020–1037 [PubMed: 23238461]
30. Hughes GA (2005) Nanostructure-mediated drug delivery. Nanomedicine 1 (1):22–30 [PubMed: 17292054]
31. Kumar B, Jalodia K, Kumar P, Gautam HK (2017) Recent advances in nanoparticle-mediated drug delivery. J Drug Deliv Sci Technol 41:260–268
32. Finnie KS, Bartlett JR, Barbé CJA, Kong L (2007) Formation of Silica Nanoparticles in Microemulsions. Langmuir 23 (6):3017–3024 [PubMed: 17300209]
33. Arriagada FJ, Osseo-Asare K (1994) Synthesis of Nanometer-Sized Silica by Controlled Hydrolysis in Reverse Micellar Systems In: Horacio EB (ed) The Colloid Chemistry of Silica. American Chemical Society, Washington, DC
34. Chia- Lu C, Scott FH (1996) Kinetics of silica particle formation in nonionic W/O microemulsions from TEOS. AICHE J 42 (11):3153–3163
35. Jaramillo N, Paucar C, García C (2014) Influence of the reaction time and the Triton x-100/ Cyclohexane/Methanol/H2O ratio on the morphology and size of silica nanoparticles synthesized via sol–gel assisted by reverse micelle microemulsion. J Mater Sci 49 (9):3400–3406
36. Soares JP, Santos JE, Chierice GO, Cavalheiro ETG (2004) Thermal behavior of alginic acid and its sodium salt. Eclet Quím 29:57–64
37. Zhuravlev LT (2000) The surface chemistry of amorphous silica. Zhuravlev model. Colloids Surf A 173 (1–3): 1–38
38. Donnan FG, Rose RC (1950) OSMOTIC PRESSURE, MOLECULAR WEIGHT, AND VISCOSITY OF SODIUM ALGINATE. Can J Res 28b (3): 105–113
39. Osseo-Asare K, Arriagada FJ (1990) Preparation of SiO2 nanoparticles in a non-ionic reverse micellar system. J Colloids Surf 50:321–339
40. Bagwe RP, Yang C, Hilliard LR, Tan W (2004) Optimization of Dye-Doped Silica Nanoparticles Prepared Using a Reverse Microemulsion Method. Langmuir 20 (19):8336–8342 [PubMed: 15350111]
41. Ab Rahman I, Padavettan V (2012) Synthesis of Silica Nanoparticles by Sol-Gel: Size-Dependent Properties, Surface Modification, and Applications in Silica-Polymer Nanocomposites-A Review. Journal of Nanomaterials. https://doi:10.1155/2012/132424
42. Lal J, Auvray L (1994) Perturbations of microemulsion droplets by confinement and adsorption of polymer. Journal de Physique II 4 (12):2119–2125.
43. Stubenrauch C (2008) Microemulsions: Background, New Concepts, Applications, Perspectives. 1st edn. Wiley-Blackwell, Hoboken, NJ
44. Siepmann J, Siepmann F (2008) Mathematical modeling of drug delivery. Int J Pharm 364 (2):328–343. [PubMed: 18822362]
45. Ritger PL, Peppas NA (1987) A simple equation for description of solute release I. Fickian and non-fickian release from non-swellable devices in the form of slabs, spheres, cylinders or discs. J Control Release 5 (1):23–36.
46. Dash S, Murthy PN, Nath L, Chowdhury P (2010) Kinetic modeling on drug release from controlled drug delivery systems. Acta Pol Pharm 67 (3):217–223 [PubMed: 20524422]
47. Li L, Li J, Si S, Wang L, Shi C, Sun Y, Liang Z, Mao S (2015) Effect of formulation variables on in vitro release of a water-soluble drug from chitosan–sodium alginate matrix tablets. Asian J Pharm Sci 10 (4):314–321.
48. Chen J, Huang G-D, Tan S-R, Guo J, Su Z-Q (2013) The Preparation of Capsaicin-Chitosan Microspheres (CCMS) Enteric Coated Tablets. Int J Mol Sci 14 (12):24305–24319 [PubMed: 24351818]
49. Cuomo F, Ceglie A, Piludu M, Miguel MG, Lindman B, Lopez F (2014) Loading and Protection of Hydrophilic Molecules into Liposome-Templated Polyelectrolyte Nanocapsules. Langmuir 30 (27):7993–7999 [PubMed: 24946085]
50. Siepmann J, Siepmann F (2012) Modeling of diffusion controlled drug delivery. J Control Release 161 (2):351–362 [PubMed: 22019555]

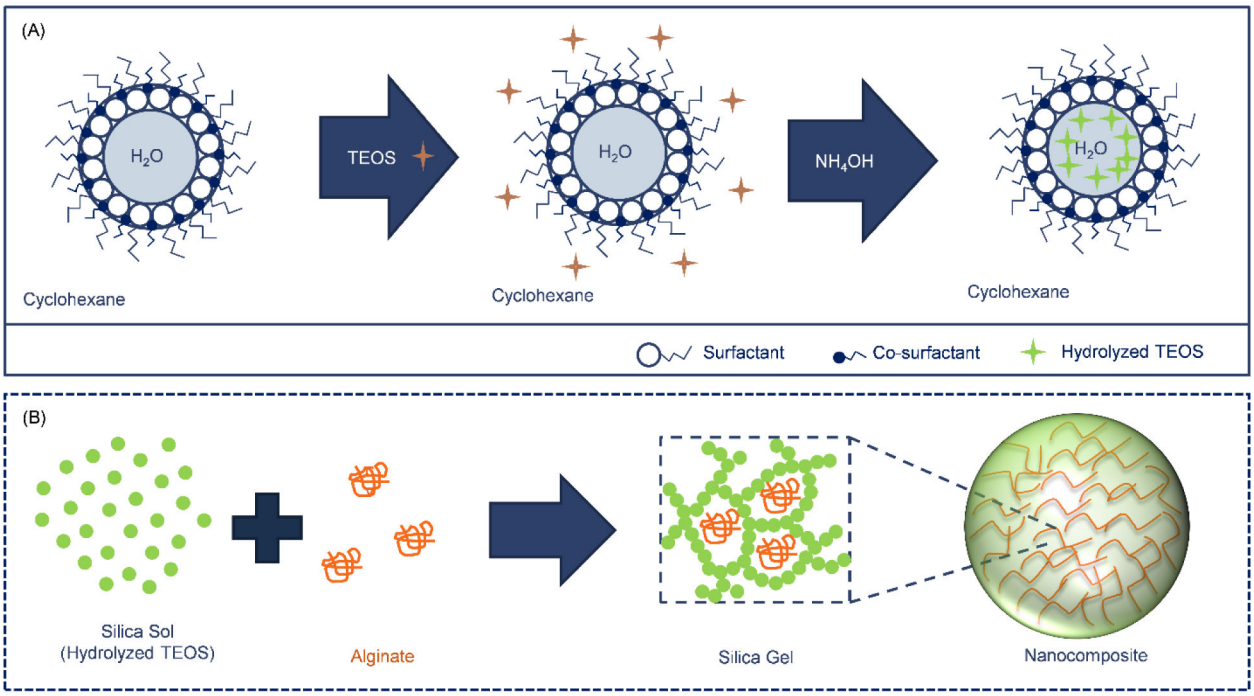

Fig. 1.

Illustration of a water-in-oil microemulsion method for entrapment of alginate within a silica sol-gel to form composite nanoparticles. (A) Initially, alginate-containing water droplets are formed, stabilized by surfactants and co-surfactants, in a cyclohexane oil phase (i.e. water-in-oil microemulsion). Upon addition, TEOS remains primarily within the oil phase due to its hydrophobicity. Addition of NH_4OH catalyzes the hydrolysis of TEOS and the formation of hydrophilic monomers that accumulate within the water droplets and nucleates the formation of suspended silica particles (i.e. a silica sol) [32, 33]. (B) Inter-particle condensation reaction leads to the formation of a silica network (i.e. sol-gel transition) with dimensions that are constrained by droplet size and precursor concentration. As the silica network grows, it could entrap any polymer (e.g. alginate) present within the water droplet.

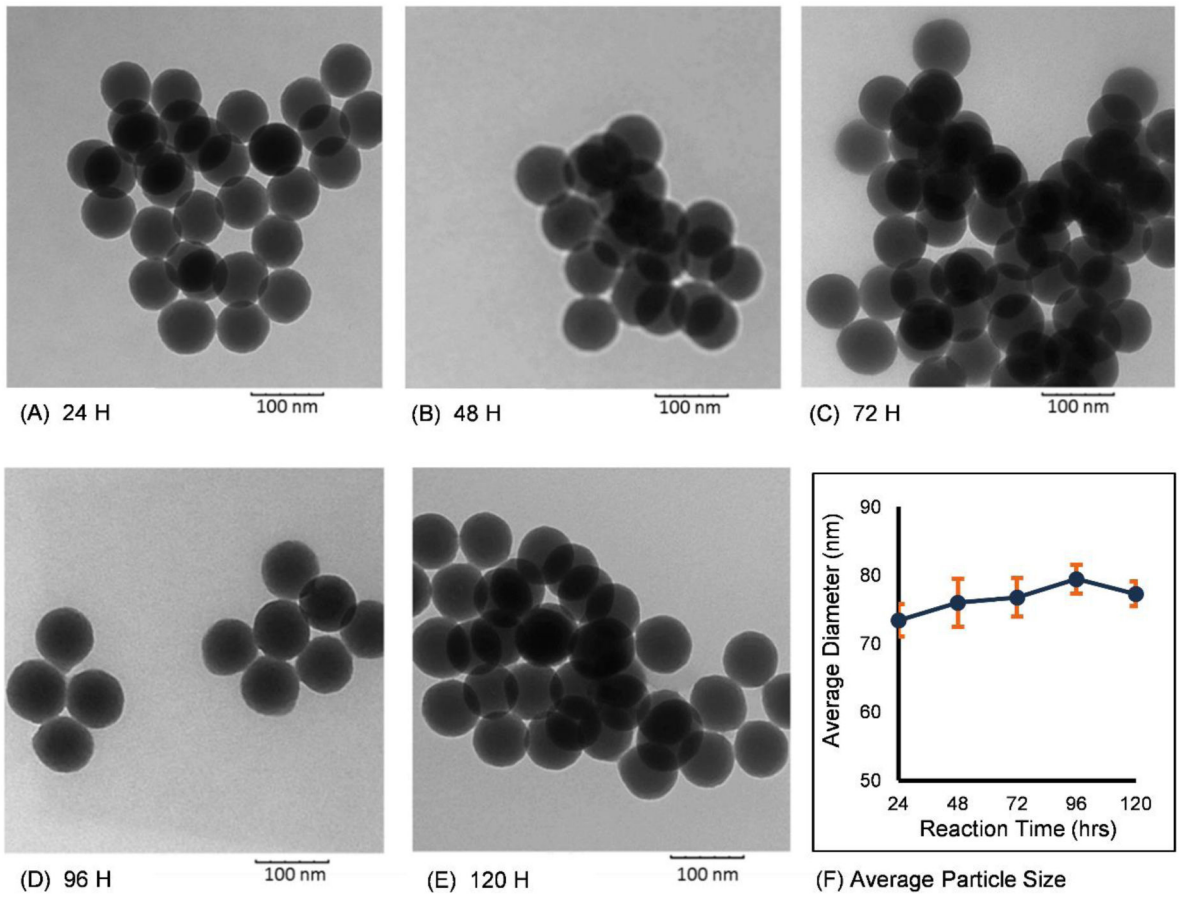

Fig. 2.

TEM images of silica-alginate nanoparticles obtained after different reaction times of: (A) 24 hours, (B) 48 hours, (C) 72 hours, (D) 96 hours and (E) 120 hours. (F) Average particle diameter, as determined from TEM images, for different reaction times.

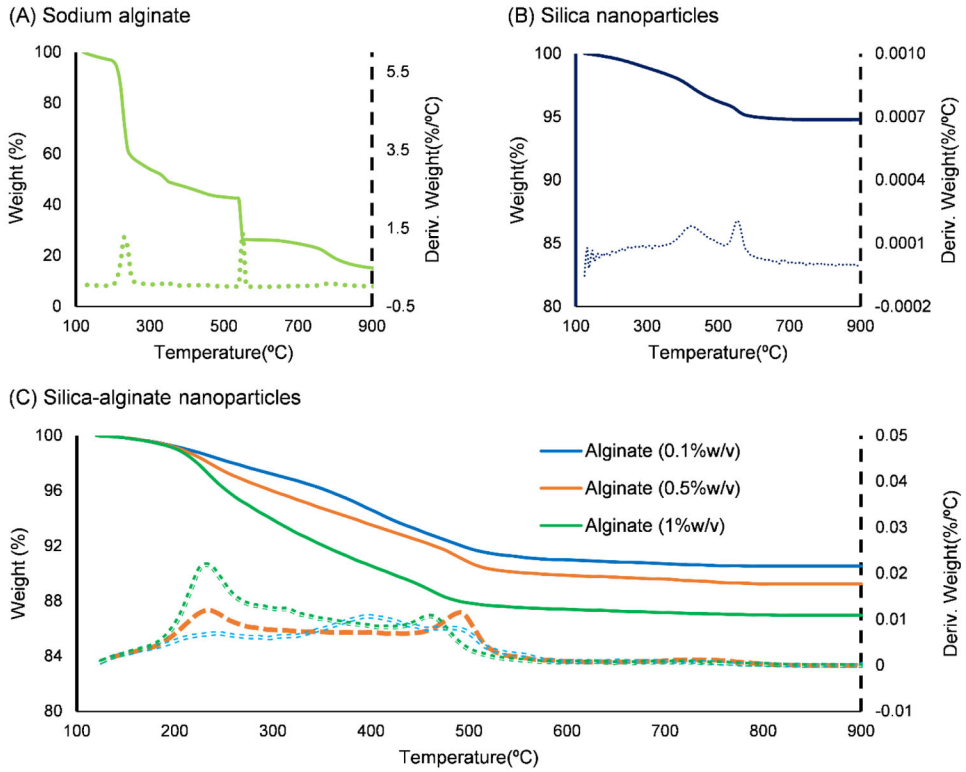

Fig. 3.

TGA (solid line) and DTGA (dash line) curves for (A) sodium alginate, (B) silica nanoparticles, and (C) silica-alginate nanoparticles produced with varying alginate concentrations used in microemulsion.

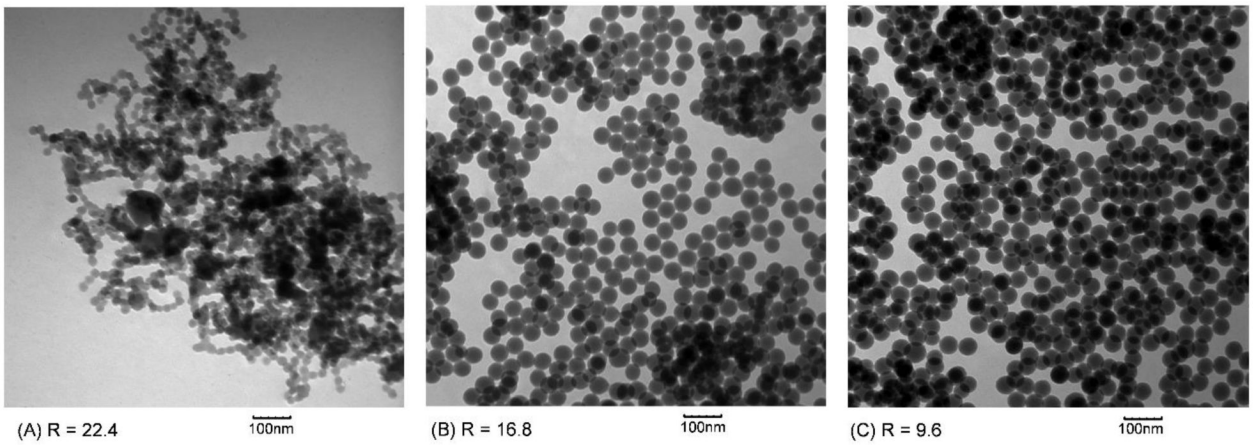

Fig. 4.

TEM images of silica-alginate nanoparticles synthesized under conditions with different *R* values of: (A) 22.4; (B) 16.8; and (C) 9.6.

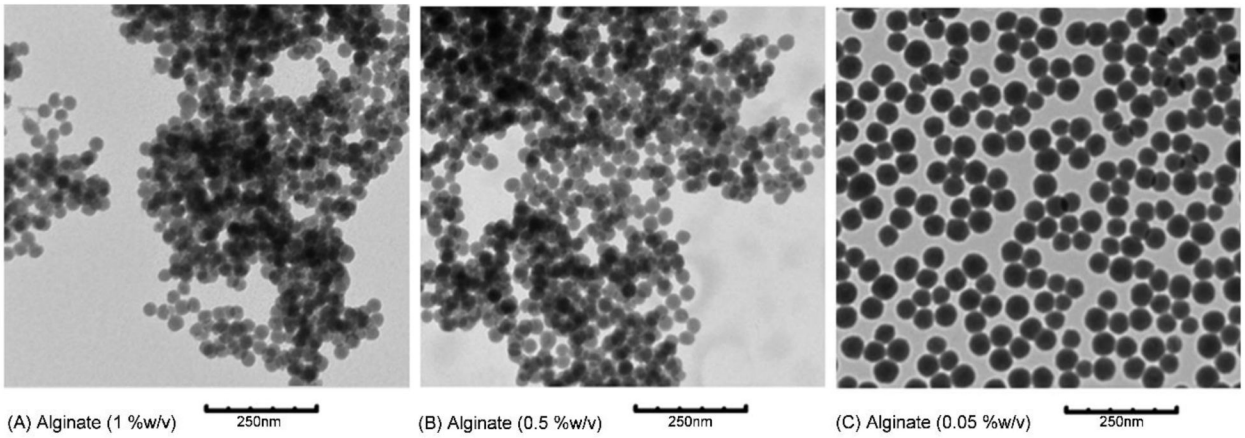

Fig. 5.

TEM images of silica-alginate nanoparticles with different initial alginate concentrations used in microemulsion. (A) alginate 1 %w/v; (B) alginate 0.5 %w/v; (C) alginate 0.05 %w/v.

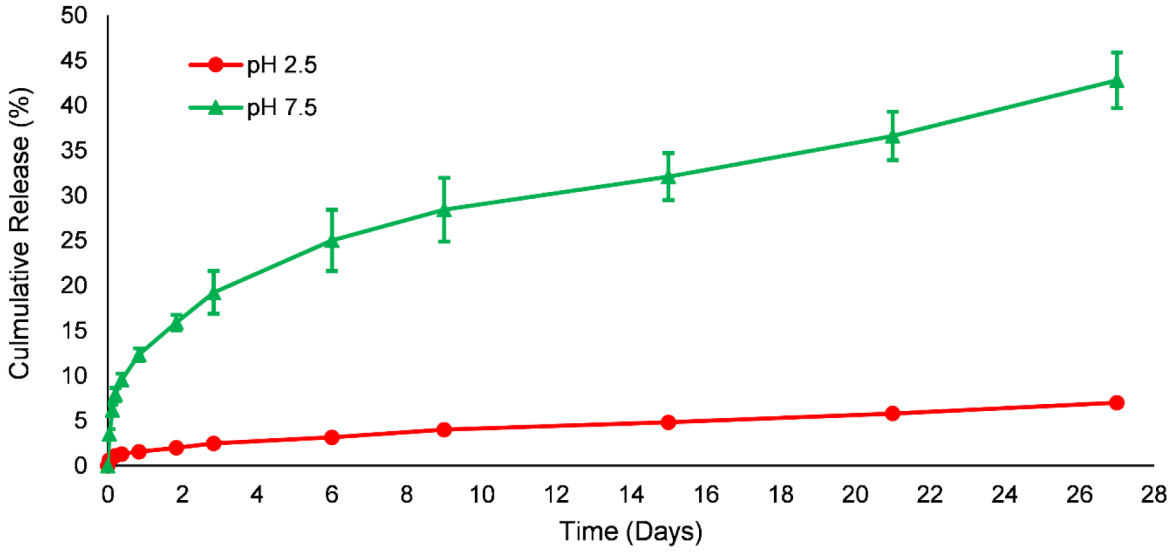

Fig. 6.

In vitro release profile of rhodamine B from silica-alginate nanoparticles in phosphate buffers at different pH values (pH 2.5 or pH 7.5). At pH 2.5, a 7 % cumulative release of rhodamine B was observed over 27 days, while 42 % cumulative release was observed at pH 7.5. (n = 3 for each experiment)

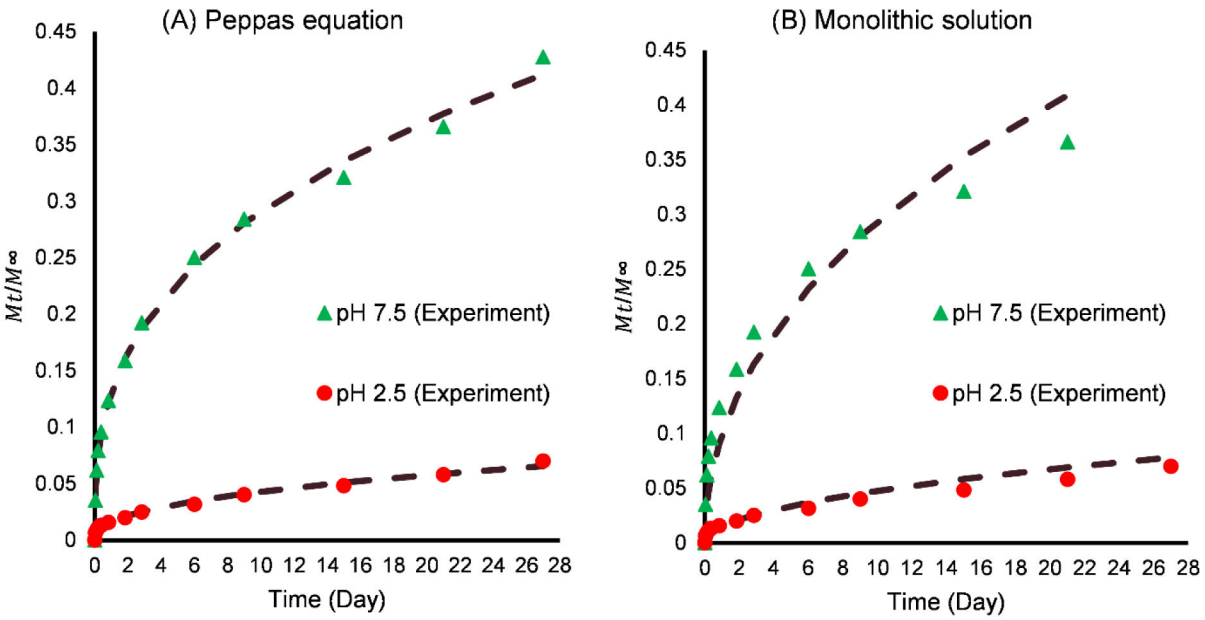

Fig. 7.

Fitting of mathematical drug release models (dash line) to experimental data of rhodamine B from in situ loaded silica-alginate nanoparticles (A) Peppas equation: pH 2.5 (R^2 = 0.9868, k = 0.016, n = 0.42); pH 7.5 (R^2 = 0.9954, k = 0.13, n = 0.35). (B) Monolithic solution: pH 2.5 (R^2 = 0.9786, D/r^2 = 0.0002); pH 7.5 (R^2 = 0.9470, D/r^2 = 0.008). (n= 3 for each experiment)

Table 1.

Water-in-oil microemulsion parameters of silica-alginate nanoparticle for different reaction time

Cyclohexane (mL)	n-hexanol (mL)	Alginate (%w/v)	Alginate (mL)	TX-100 (mL)	TEOS (mL)	NH_4OH (mL)
15	3.6	0.1	1	3.6	0.5	0.12

Table 2.

Water-in-oil microemulsion parameters of silica-alginate nanoparticle for TGA analysis

Cyclohexane (mL)	n-hexanol (mL)	Alginate (%w/v)	Alginate (mL)	TX-100 (mL)	TEOS (mL)	NH_4OH (mL)
60	12	0.1	4	10	2	0.5
60	12	0.5	4	10	2	0.5
60	12	1.0	4	10	2	0.5

Table 3.

Variation of composite particle size with R values

Cyclohexane (mL)	n-hexanol (mL)	Alginate[a] (mL)	TX-100 (mL)	TEOS (mL)	NH_4OH (mL)	$R = \frac{[H_2O]}{[TX-100]}$	Particles Size(nm)
60	7.2	4	6	1	0.5	22.4	24.3 ± 2.4
60	9.6	4	8	1	0.5	16.8	39.0 ± 3.1
60	16.8	4	14	1	0.5	9.6	49.3 ± 3.3

[a]: 0.05%w/v alginate solution

Table 4.

Particle size variation associated with initial alginate concentration used in microemulsion ($R = 5.6$)

Cyclohexane (mL)	n-hexanol (mL)	Alginate (%w/v)	Alginate (mL)	TX-100 (mL)	TEOS (mL)	NH_4OH (mL)	Particles Size(nm)
80	30	1	7.5	45	1.5	0.6	37.3 ± 3.4
80	30	0.5	7.5	45	1.5	0.6	42.0 ± 2.9
80	30	0.05	7.5	45	1.5	0.6	57.2 ± 5.7